IOP Conf. Series: Materials Science and Engineering **161** (2016) 012049 doi:10.1088/1757-899X/161/1/012049

An Energy-Critical Plane Based Fatigue Damage Approach for the Life Prediction of Metal Alloys

N Pitatzis[1] and G Savaidis[1]

[1]Department of Mechanical Engineering, Aristotle University of Thessaloniki, GR-54124 Thessaloniki/Greece

E-mail: pitatzis@auth.gr

Abstract. This paper presents a new energy-critical plane based fatigue damage approach for the assessment of the fatigue life under uniaxial and multiaxial proportional and non-proportional fatigue loading. The proposed approximate method, based on Farahani's multiaxial fatigue damage model, takes into account the critical plane orientations during a loading cycle and the values of the respective damage parameters on them. The uniqueness of the proposed method lies on the fact that it considers a weighted contribution of each critical plane orientation to the material damage. The relative weighting factors depend on the declination of each critical plane with respect to the critical plane, where the damage parameters exhibit their maximum values during a fatigue loading cycle. Herein, several low, mid and high-cycle fatigue loading cases are being investigated. The induced elastic-plastic stress-strain states are approximated by means of respective finite element analyses (FEA). Several experimental fatigue data derived from uniaxial and multiaxial fatigue tests on StE460 steel alloy thin-walled hourglass-type specimens have been used to verify the model's calculation accuracy. Comparison of experimental and calculated fatigue lives confirm remarkable fatigue life calculation accuracy in all cases examined.

1. Introduction

The need for lightweight, safe and financially optimized engineering systems performing under fatigue loading implies an in-depth investigation of the physical phenomena related to the loss of structural integrity, and the establishment of respective mathematical methods for the approximate calculation of structural durability. During the last three decades the research interest on Fatigue has been focused on the multiaxial case [1, 2, 3, 4, 5] as a one-way path to attain lighter and even safer structures. This is due to the fact that in the case of multiaxial fatigue, neither the physical phenomena related to the damage of the material have been thoroughly investigated, nor the former mathematical material constitutive models were proven to lead to results of satisfactory accuracy [6, 7, 8, 9]. The effort on multiaxial fatigue could be distinguished into two major research fields, namely the pursuit for the establishment of new, reliable material models to approximate the elastic-plastic multiaxial stress-strain state [1, 10, 11, 12] and the challenge for the constitution of fatigue damage approach methods in order to attain credible approximation of fatigue life [13, 14, 15, 16, 17, 18].

This work focuses on the second field of fatigue life approach and incorporates a proposed multiaxial fatigue criterion established on energy-critical plane basis. The assessment of multiaxial fatigue life can be achieved via three potential paths; stress, strain and energy-based approaches. It has been referred [16] that for all the above-mentioned fatigue life assessment methods, when the damage parameters are being considered on the critical planes, then the respective approximate methods lead to the most satisfactory results. Furthermore, energy based approaches are proven to be the less parameter-demanding methods [17, 18, 19] compared to stress and strain based approaches so as for contiguous fatigue life approximation accuracy to be achieved. These facts constitute important incentives for further research towards energy-critical plane based fatigue assessment methods, as disclosed herein.

2. The proposed energy-critical plane fatigue damage approach

The significance of using energy-based fatigue damage parameters considered on critical planes lies on the fact that these planes and the energy conveyed on them are being directly related to the physical causes of materials' failure due to fatigue [20, 21]. According to Taylor [22], the deformation of solid materials under external loading results from the dislocation movement detected on atomic scale due to shear stresses acting on crystal lattice planes with the minimum shear strength. Accordingly, it is proved [23, 24] that the initiation of material consistency degradation under fatigue loading is being detected on plane orientations where shear stresses and strains attain their maximum values. Figure 1 shows a thin-walled hourglass specimen subjected to combined axial-torsional loading with time varying axial force F and torsional moment M_T, as well as the local plane stress on the highlighted finite free surface of the specimen on a specific moment, the corresponding critical plane orientation where shear stress, τ_{yz}, reaches its maximum value, τ_{max}, the perpendicular to the critical plane normal stress component, σ_n, responsible for the propagation of the failure and the corresponding maximum shear and normal strain, γ_{max} / 2 and ε_n respectively.

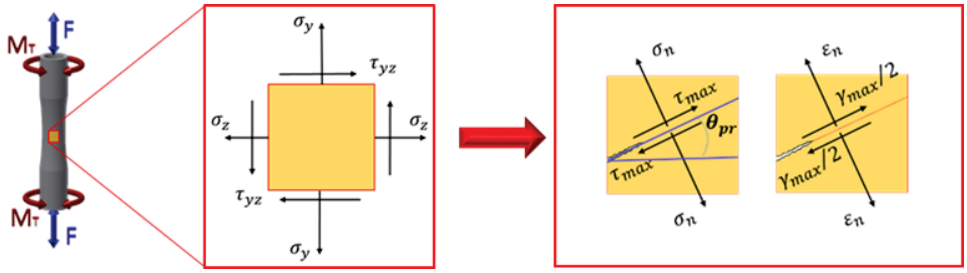

Figure1. Critical plane derived from a given plane stress state and respective critical plane orientation angle, θ_{pr}.

The magnitude of τ_{max} and σ_n and the extend of non-proportionality in conjunction with the microstructure of the material [25] are the major parameters related to the materials' durability under fatigue loading. The critical plane orientation could be defined according to the stress transformation formulas of Mohr, applicable to both uniaxial and multiaxial stress states [17]. When combined fatigue loading components are being applied, the orientation of the critical plane alters by time. In the case of non-proportional fatigue this alternation becomes prominent compared to the corresponding critical plane orientation changes under proportional loading with the same nominal stress amplitudes as shown in figure 3.

Taking all the above into account, the proposed fatigue life approximate method is being implemented according to the following steps:

1st step: Calculation of local elastic-plastic strains and stresses.

The stress-strain state is being approximately calculated by means of respective elastic-plastic FEA on the external free surface of smooth, thin-walled, hourglass-type specimens made of StE460 steel alloy. The von Mises yield criterion [26] in conjunction with the non-linear kinematic hardening model of Chaboche [27] are being applied. The geometrical parameters of the specimen and the mechanical properties of the material under investigation are being included in Table 1. The geometrical characteristics of the specimen and a representative finite element mesh configuration are shown in figure 2.

Axisymmetric solid elements (SOLID273, [28]) have been applied to model the axisymmetric solid structure. The elements are being defined by eight nodes on a master plane and the rest of the nodes are being automatically defined in the circumferential direction based on the eight master plane nodes. Each element node has three degrees of freedom, namely the translations on the x, y and z directions. A total number of 1065 elements, with a minimum length of 0.1mm detected on the z axis, progressively increasing as the distance from the xz plane increases to reach the maximum length of 5.5mm, have been used for the creation of the finite element mesh (figure 2).

Table 1. Geometrical data of the thin-walled, hourglass-type specimens and mechanical properties of steel StE460 [29, 30].

Geometrical Parameters					
$D_o(mm)$	$D_i(mm)$		$D_h(mm)$	$R(mm)$	$H(mm)$
50	41		36	130	220
Mechanical Properties					
$R_m[MPa]$	$R_{p0.2}\,[MPa]$	$E\,[MPa]$	v	$K'[MPa]$	n'
643	500	208500	0.3	1115	0.161
ε_f'	$\sigma_f'\,[MPa]$	γ_f'	$\tau_f'\,[MPa]$	c	b
0.281	969.6	1.87	585	-0.493	-0.086

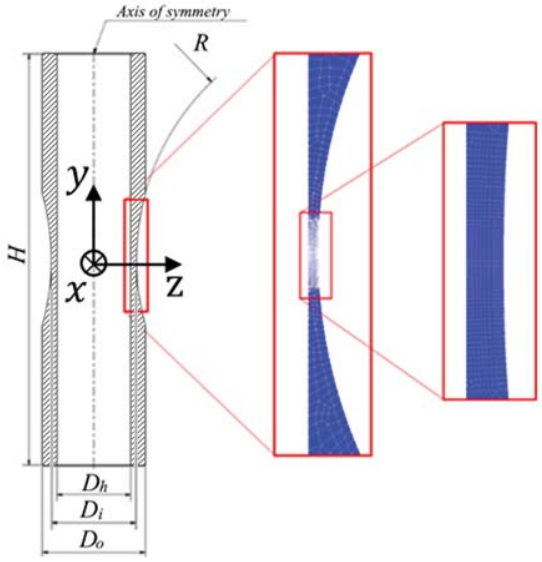

Figure 2. Thin-walled hourglass type specimen and typical finite element mesh configuration.

The normal stress-normal strain and the shear stress-shear strain stabilized hystereses derived from FEA after five (5) fatigue cycles are being used for the assessment of the respective fatigue life according to the proposed fatigue life assessment method. Significant engineering parameters used in the framework of the present work are the nominal normal and shear stresses, ***S*** and ***T*** respectively, which are being defined according to Ref. [31], as follows:

$$S = \frac{F}{\pi\left(\left(D_i{}^2 - D_h{}^2\right)/4\right)} \tag{1}$$

$$T = \frac{2M_T}{\pi\left(\left(D_i{}^3 - D_h{}^3\right)/8\right)} \tag{2}$$

2nd step: Calculation of fatigue damage parameters.

Two fatigue damage parameters, Π_I and Π_{II}, have been implemented, namely the product of the maximum shear stress and the respective maximum shear strain on the critical plane, relative to the critical plane orientation, θ_{pr}:

$$\Pi_I = \left[\tau_{max} \cdot \left(\frac{\gamma_{max}}{2}\right)\right](\theta_{pr}), \tag{3}$$

and the product of the normal to the critical plane stress and the respective normal strain relative to the critical plane orientation, θ_{pr} (figure 1),

$$\Pi_{II} = [\sigma_n \cdot \varepsilon_n](\theta_{pr}). \tag{4}$$

Given the stabilized stress-strain hysteresis loops derived from the FEA according to the first step, the calculation of the before-mentioned parameters becomes feasible for a full fatigue cycle. The bandwidth of possible critical plane orientations ($-45° \leq \theta_{pr} \leq 45°$) is being divided into orientation segments of 5 degrees ($\Delta\theta_{pr} = 5°$) and the sum of each damage parameter, Π_I and Π_{II} is being calculated for each 5-degree segment and for a full loading cycle. A typical distribution of $\sum_T \Pi_I(\Delta\theta_{pr})$ and $\sum_T \Pi_{II}(\Delta\theta_{pr})$ during a fatigue cycle under proportional and non-proportional fatigue, where combined axial and torsional loading components are being applied, are shown in the qualitative bar diagrams of figure 3a and 3b, respectively, where the significant difference between the two distributions is prominent.

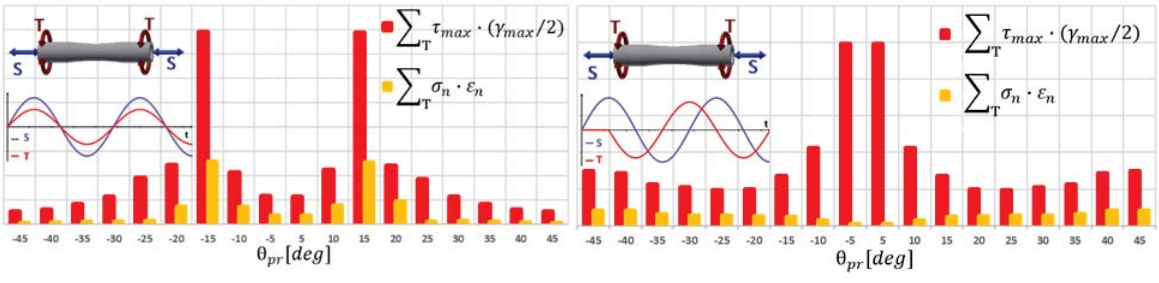

Figure 3. Qualitative bar diagrams of $\sum_T \Pi_I(\Delta\theta_{pr})$ and $\sum_T \Pi_{II}(\Delta\theta_{pr})$ distribution during a full loading cycle under (a) proportional and (b) non-proportional fatigue, where combined sinusoidal axial and torsional loading components with the same nominal stress amplitudes ($S_{a,prop} = S_{a,non-prop}$ and $T_{a,prop} = T_{a,non-prop}$) and phase differences of $\Delta\varphi = 0°$ and $\Delta\varphi = 90°$ respectively are being applied.

3nd step: Introduction of fatigue damage weighting factors.

Taking into consideration the maximum shear stress-critical plane approach [13, 15], the 5-degree critical plane orientation bandwidth, where $\sum_T \boldsymbol{\Pi_{II}(\Delta\theta_{pr})}$ attains its maximum value, is the one where the fatigue crack is more likely to be induced. According to the proposed fatigue life approximate method, the contribution to the material damage of $\sum_T \boldsymbol{\Pi_{II}(\Delta\theta_{pr})}$ parameter on the rest 5-degree segment orientations is being decreased -by the introduction of a relative damage weighting factor- as the declination of each critical plane with respect to the critical plane where the damage parameters exhibit their maximum values increases. The physical explanation of this assessment lies on the fact, that the normal stress on other critical planes than the one where the crack is expected to be induced, could not contribute to the crack opening-closure -and accordingly to fatigue damage- at the same extend, because of the declination between the orientation of the theoretical crack propagation plane and the several critical plane orientations that significantly deviate from the critical plane orientation 5-degree bandwidth where $\sum_T \boldsymbol{\Pi_{II}(\Delta\theta_{pr})} = \boldsymbol{max}$, as shown in figure 4. It is plausible that this contribution lessens for critical planes with larger declination with respect to the orientation, where $\sum_T \boldsymbol{\Pi_{II}(\Delta\theta_{pr})} = \boldsymbol{max}$. The following weighting factor is proposed to describe this assumption mathematically:

$$W_{f\sigma,i} = 1 - i\left(\frac{1}{9}\right),\ i = 1, \dots, 8 \tag{5}$$

Each weighting factor $\boldsymbol{W_{f\sigma,i}}$ acts as a multiplier on each respective sum, $\sum_T \boldsymbol{\Pi_I(\Delta\theta_{pr})}$ as depicted in figure 4.

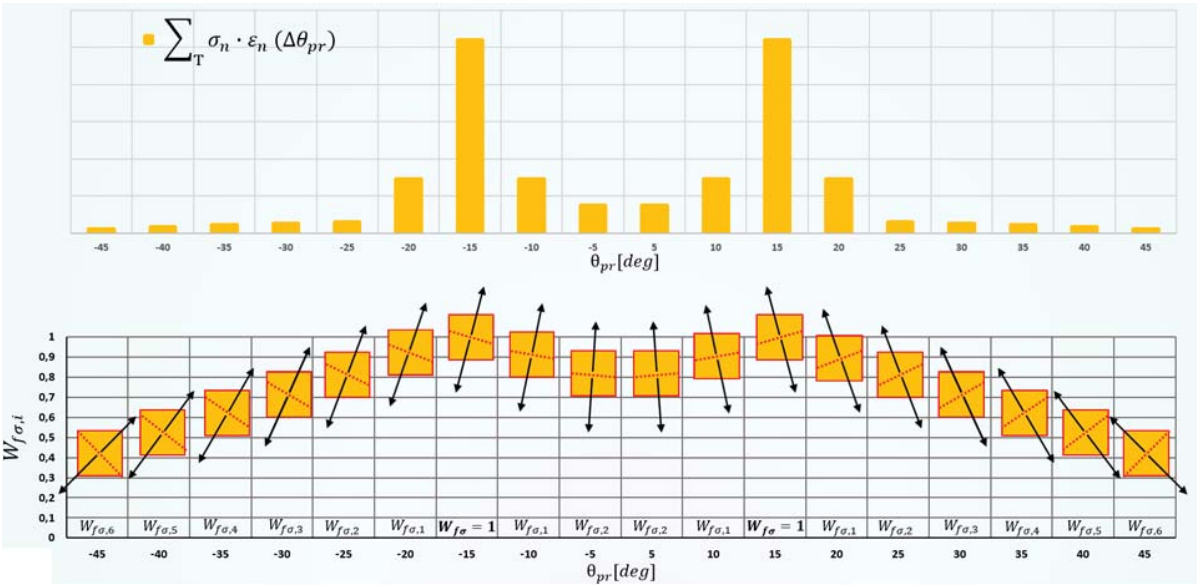

Figure 4. Qualitative bar diagram of $\sum_T \Pi_{II}(\Delta\theta_{pr})$ distribution during a fatigue cycle (up), critical plane orientations susceptible to crack initiation, where $W_{f\sigma,i} = 1$, and $W_{f\sigma,i}$ values distribution for each 5-degree critical plane orientation segment (down).

Furthermore, a second fatigue damage weighing factor, $\lambda_{\sigma_{n,max,i}}$ is being introduced, which equals the ratio of the maximum value of σ_n identified on each 5-degree critical plane orientation segment over the stress that corresponds to strain value of 0.2%, considering the stabilized stress-strain curve of the material

under cyclic fatigue loading. Considering this, $\lambda_{\sigma_{n,max,i}}$ is calculated for each 5-degree critical plane orientation bandwidth according to the equation:

$$\lambda_{\sigma_{n,max,i}} = \frac{\sigma_{n,max,i}}{\sigma_{\varepsilon=0.2\%}}, i = 1, \dots, 9 \quad (6)$$

Each one of the nine weighting factors, $\lambda_{\sigma_{n,max,i}}$, acts as a multiplier on each respective sum, $\sum_T \Pi_I(\Delta\theta_{pr})$. Eqs. (5) and (6) have been derived from several parametrical fatigue life assessment analyses, and after comparative studies with corresponding uniaxial and multiaxial fatigue test data [24], that have been accomplished in order to attain the most reliable fatigue life assessment.

4th step: Fatigue life assessment.

Taking into account the above mentioned fatigue damage weighting factors and the concept of Farahani (Fa) [17, 18] the following equation for the approximate calculation of fatigue life is being proposed:

$$\frac{(1+\frac{\sigma_n^m}{\sigma_f'})}{(\tau_f' \gamma_f')}\left(\Sigma\Pi_I(\Delta\theta_{pr,\tau,1})\right)+\lambda_{\sigma_{n,max,1}} W_{f\sigma,1}\frac{1}{(\sigma_f' \varepsilon_f')}\left(\Sigma\Pi_{II}(\Delta\theta_{pr,\sigma n,1})\right)+\dots+\frac{(1+\frac{\sigma_n^m}{\sigma_f'})}{(\tau_f' \gamma_f')}\left(\Sigma\Pi_I(\Delta\theta_{pr,\tau,9})\right)+$$
$$\lambda_{\sigma_{n,max,9}} W_{f\sigma,9}\frac{1}{(\sigma_f' \varepsilon_f')}\left(\Sigma\Pi_{II}(\Delta\theta_{pr,\sigma n,9})\right) = \left(\frac{\sigma_f'}{E}(N_f)^b + \varepsilon_f'(N_f)^c\right) + \left(\frac{\tau_f'}{G}(N_f)^b + \gamma_f'(N_f)^c\right) \quad (7)$$

It should be noted that when $W_{f\sigma,i}$ and $\lambda_{\sigma_{n,max,i}}$ take unit values, the expression (7) yields Farahani's equation [17]. The qualitative effect of the implementation of $W_{f\sigma,i}$ and $\lambda_{\sigma_{n,max,i}}$ to the fatigue life assessment according to Eq. (7) is depicted in figure 5. It should be noted that the Wöhler curves shown in figure 5 are qualitative and indicative and are only used to illuminate on the effect of the proposed fatigue damage weighting factors to the approximate fatigue life calculations. Nonetheless an indicative fatigue limit (parallel to the N_f axis segment of the indicative curves) is being used, given that the material under study (StE460 steel alloy) exhibits fatigue limit [31].

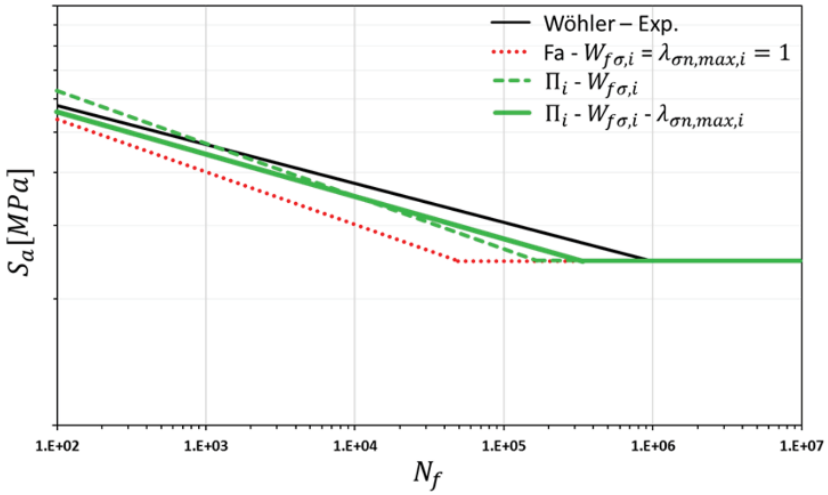

Figure 5. Qualitative illustration of the influence of the implementation of the damage weighting factors $W_{f\sigma,i}$ and $\lambda_{\sigma_{n,max,i}}$ on the Wöhler curve position in comparison to the Wöhler curve calculated using Farahani's concept.

Specifically, the introduction of solely the proposed weighting factor, $W_{f\sigma,i}$, (dashed green curve in figure 5) leads to the assessment of longer fatigue life, compared to that calculated if $W_{f\sigma,i}$ is not considered (red dotted line = Farahani's concept). Practically, the use of the weighting factor, $W_{f\sigma,i}$, leads to parallel shift of the Wöhler curve calculated using Farahani's model to higher fatigue lives. Consequently, the contribution of $W_{f\sigma,i}$ to the fatigue life calculation eliminates the reported disadvantage of Farahani's model to underestimate fatigue life in the regime of high cycle fatigue [19].

$\lambda_{\sigma_{n,max,i}}$ yields the rotation of the Wöhler curve counter-clockwise as qualitatively shown in figure 5. It acts as corrective factor that leads to more reliable fatigue life assessment in the of low cycle fatigue regime. Thereafter, the introduction of both fatigue damage weighting factors, $W_{f\sigma,i}$ and $\lambda_{\sigma_{n,max,i}}$, to the fatigue life calculation, as proposed herein, yields the thick green-coloured Wöhler curve shown in figure 5.

3. Evaluation of the proposed method and future perspectives

The here proposed energy-critical plane based fatigue damage approach for the life prediction of metal alloys has been evaluated through comparison with corresponding experimental results. In particular, four fatigue loading categories have been examined; uniaxial tension-compression, pure torsion, multiaxial proportional and non-proportional cyclic loading with combined tension – torsion components [24]. Table 2 gives a summarizing overview of the theoretical and experimental results and corresponding % logarithmic errors, $E_{er}(\%)$, where

$$E_{er}(\%) = \log\left(\frac{N_{f,predicted}}{N_{f,experimental}}\right)(\%) \tag{8}$$

for the loading cases investigated are included in Table 2.

Table 2. Loading data for all cyclic fatigue cases examined, experimental and calculated fatigue lives according to the proposed and Farahani's method, and respective % logarithmic errors.

Loading	S_a [MPa]	T_a [MPa]	$_d$	$N_f - EXP$	$N_f - \Pi_i$	$N_f - Fa$	$E_{er}(\%) - \Pi_i$	$E_{er}(\%) - Fa$
Tension-Compression	338.8	-	-	50100	42556	22123	-7.08	-35.49
	385	-	-	7690	6921	4614	-4.57	-22.18
	450.2	-	-	1630	1888	912	6.38	-25.21
Pure Torsion	-	204	-	38250	31112	31112	-8.97	-8.97
	-	212.7	-	23000	19182	19182	-7.88	-7.88
	-	257.5	-	1820	2433	2433	12.60	12.60
Tension-Torsion Proportional	172.2	137.4	0	130300	103714	75801	-9.91	-23.52
	216.5	147.3	0	521000	410502	325587	-10.35	-20.41
	244.2	147.3	0	31100	24880	17416	-9.69	-25.18
Tension-Torsion non-Proportional	215	149.2	90	574600	295885	133585	-28.82	-63.36
	295	193.4	90	51900	32178	16089	-20.76	-50.86
	318.8	184.2	90	39670	29752	15074	-12.49	-42.02
	391.5	230.9	90	6570	5626	2811	-6.73	-36.87
	480.9	269.3	90	540	480	210	-5.06	-40.89

Figures 6 to 9 contain comparative illustration of the results. Therein, the calculation results obtained from the proposed model are illustrated with triangle shaped symbols. The respective fatigue lives derived from Farahani's model, i.e. Eq. (7) considering $W_{f\sigma,i} = \lambda_{\sigma_{n,max,i}} = 1$, are represented with circle spots. Square symbols are used for the corresponding experimental data. In all fatigue loading cases studied, the approximate fatigue life results attained from the proposed method (Π_i) led to fatigue life prediction of

better accuracy compared to the respective accuracy derived from Eq. (7) if no fatigue damage weighting factors are being considered (Farahani concept). The characteristic coincidence between results derived from the proposed method and the method based on the concept of Farahani is also distinguishable in the case of pure torsion (figure 7), due to the theoretically zero value of the perpendicular to the critical plane normal stress component, σ_n.

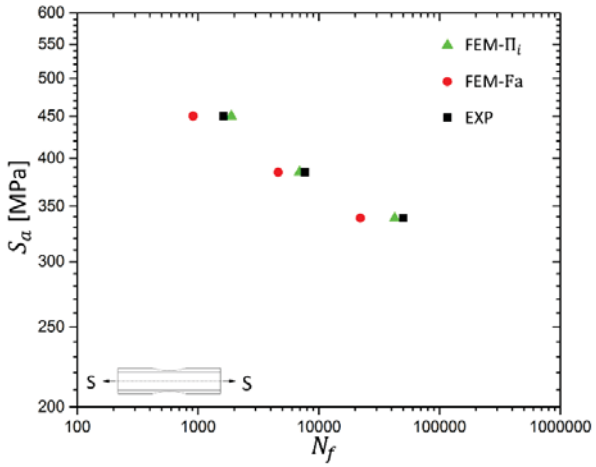

Figure 6. Experimental (EXP) and corresponding calculated fatigue lives according to the proposed method (FEM-Π_i) and Farahani's model (FEM-Fa) for constant amplitude tension-compression cyclic fatigue loading.

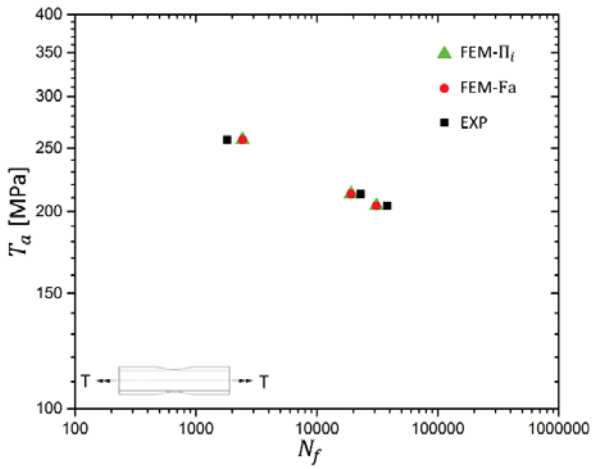

Figure 7. Experimental (EXP) and corresponding calculated fatigue lives according to the proposed method (FEM-Π_i) and Farahani's model (FEM-Fa) for pure torsion cyclic loading.

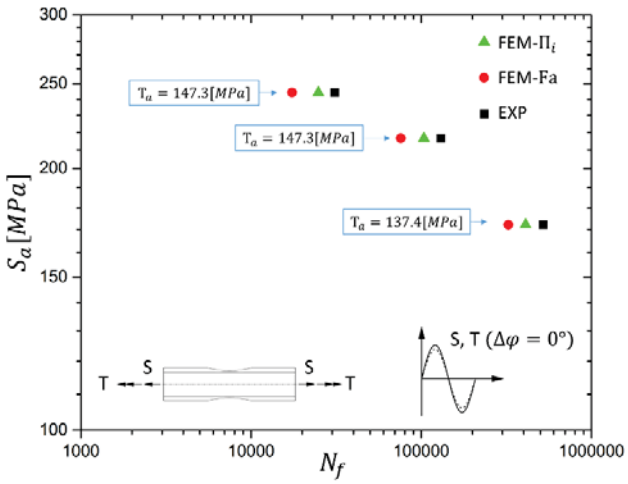

Figure 8. Experimental (EXP) and corresponding predicted fatigue lives according to the proposed method (FEM-Π_i) and Farahani's model (FEM-Fa) for proportional tension-torsion cyclic loading.

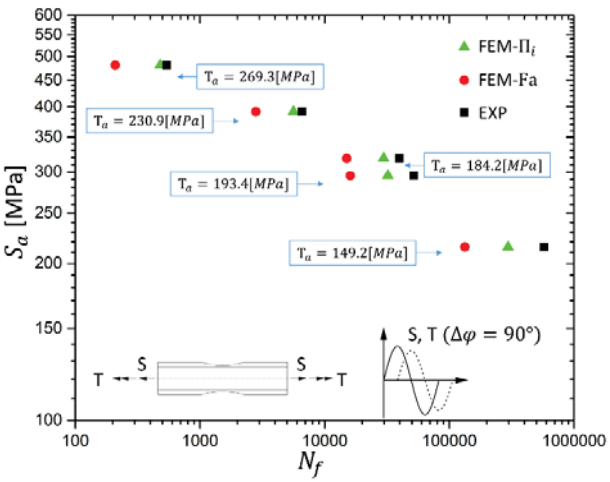

Figure 9. Experimental (EXP) and corresponding predicted fatigue lives according to the proposed method (FEM-Π_i) and Farahani's model (FEM-Fa) for non-proportional tension-torsion cyclic loading.

The first significant advantage of the proposed method lies in the fact that it introduces a weighted contribution to fatigue damage of the normal stress and strain that act perpendicular to the critical plane. This is achieved by mapping the damage parameters Π_I and Π_{II} through a full fatigue cycle not only as far as their values is concerned, but also taking into account their corresponding values as a function of the critical plane orientation angle, θ_{pr}. The combined implementation of the proposed damage weighting factors $W_{f\sigma,i}$ and $\lambda_{\sigma_{n,max,i}}$ aims at the mathematical description of respective physical phenomena related to the loss of structural integrity due to fatigue. In particular:

- $W_{f\sigma,i}$ covers the influence of the critical plane orientation shift (figure 3 and 4) to fatigue life. Herein, this influence is not regarded only as a function of the accumulated damage induced by the effect of σ_n and ε_n to the crack propagation on several critical plane orientations during a loading cycle, but also as a function of the divergence between each critical plane orientation and the critical plane where the crack due to fatigue is more likely to be induced.
- $\lambda_{\sigma_{n,max,i}}$ describes the material's sensitivity to micro crack propagation due to fatigue under the influence of σ_n and ε_n, related to the strain limit where plastic deformation becomes prominent under cyclic loading ($\sigma_{\varepsilon=0.2\%}$). According to the proposed concept the material experiences structural integrity loss under the influence of σ_n and ε_n that is not just proportional to the value of the relative damage parameter $\Pi_{II} = [\sigma_n \cdot \varepsilon_n](\theta_{pr})$ but is also proportionally affected by the ratio of σ_n over the stress value that corresponds to the barrier over which significant plastic strain occurs under cyclic loading ($\sigma_{\varepsilon=0.2\%}$). Therefore, the incorporation of fatigue damage weighting factor $\lambda_{\sigma_{n,max,i}}$ acts as a sensitivity parameter that induces more damage per fatigue cycle in the regime of low cycle fatigue and as damage alleviator in the regime of high cycle fatigue, leading to fatigue life approximations of better accuracy.

Another worth-mentioning advantage of the proposed method is that its implementation requires the same minimum -compared to corresponding multiaxial fatigue damage models [19]- number of material parameters as in the case of Farahani's model, while, in parallel, the calculation of the proposed weighting factors' values does not require additional material parameters.

Nonetheless it should be pinpointed that further evaluation of the proposed model's reliability on other materials and additional loading cases is also required. Accordingly, and taking into account that StE460 belongs to the category of cyclic softening materials, the investigation of the approximation accuracy of the proposed method in the case of cyclic hardening materials, for instance Al5083, is a scope of great significance. Presently, the authors work on the extension of the model's applicability to notched components, where stress concentration, stress gradients and surface treatment are also to be taken into account.

4. Conclusions

A reliable, easily applicable energy-critical plane based fatigue damage approach for the life prediction of metal alloys has been developed based on the model of Farahani [17, 18]. In all fatigue loading cases examined, it was proven that the proposed method yields approximate fatigue lives of remarkable accuracy. The advantage of the proposed method lies on the fact that, all the material parameters needed for its implementation are available in the bibliography [31] and the proposed damage weighting factors can be analytically approximated for other materials according to the procedure followed here, in the case of StE460. In the framework of the present work the finite element method has been applied to approximate the stress-strain elastic-plastic state. Significant incentives for relative future work are the perspective to upgrade the proposed model to become applicable on notched components as well as its combination with analytical methods for the approximate calculation of the stress-strain state under multiaxial fatigue, as an alternative to the finite element method.

References

[1] M. Hoffmann and T. Seeger, A Generalized Method for Estimating Multiaxial Elastic–Plastic Notch Stresses and Strains, *J. Eng Mater Tech*. **107** (1985) 250-254.
[2] R. Yuuki, K. Akita and N. Kishi, The effect of biaxial stress state and changes of state on fatigue crack growth behavior, *International Journal of Fatigue*. **12** (1989) 93-103.
[3] C. C. Chu, Multiaxial fatigue life prediction method in the ground vehicle industry, *International Journal of Fatigue*. **19** (1997) 325-330.
[4] B. Li, L. Reis and M. De Freitas, Simulation of cyclic stress/strain evolutions for multiaxial fatigue life prediction, *International Journal of Fatigue.* **28** (2006) 451-458.
[5] A. K. Marmi, A. M. Habraken and L. Duchene, Multiaxial fatigue damage modelling at macro scale of Ti–6Al–4V alloy, *International Journal of Fatigue.* **31** (2009) 2031-2040.
[6] C. A. Gonçalves, J. A. Araújo and E. N. Mamiya, Multiaxial fatigue: A stress based criterion for hard metals, *International Journal of Fatigue.* **27** (2005) 177-187.
[7] D. F. Socie, Critical plane approaches for multiaxial fatigue damage assessment, *Advances in Multiaxial Fatigue, STP 1191, Philadelphia, ASTM*. (1993) 7-36.
[8] C. H. Wang and M. W. Brown, Life prediction techniques for variable amplitude multiaxial fatigue—Part 1: Theories, *J. Eng. Mater. Technol.* **118** (1996) 367-370.
[9] T. Itoh, T. Nakata, M. Sakane and M. Ohnami, Nonproportional low cycle fatigue of 6061 aluminum alloy under 14 strain paths, *European Structural Integrity Society.* **25** (1999) 41-54.
[10] R. Döring, J. Hoffmeyer, T. Seeger and M. Vormwald, A plasticity model for calculating stress–strain sequences under multiaxial nonproportional cyclic loading, *Computational Materials Science.* **28** (2003) 587-596.
[11] I. V. Papadopoulos, et al., A comparative study of multiaxial high-cycle fatigue criteria for metals, *International Journal of Fatigue.* **19** (1997) 219-235.
[12] T. Palin-Luc and S. Lasserre, High cycle multiaxial fatigue energy criterion taking into account the volume distribution of stresses, Elsevier, *European Structural Integrity Society.* (1999) 115-129.
[13] A. Fatemi and D. F. Socie, A critical plane approach to multiaxial fatigue damage including out-of phase loading, *Fatigue & Fracture of Engineering Materials & Structures.* **11** (1998) 149-165.
[14] S. E. Onome, et al., A new distortion energy-based equivalent stress for multiaxial fatigue life prediction, *International Journal of Non-Linear Mechanics.* **47** (2012) 29-39.
[15] D. L. McDiarmid, A shear stress based critical-plane criterion of multiaxial fatigue failure for design and life prediction, *Fatigue Fract. Eng. Mater. Struct.* **17** (1995) 1495-1484.
[16] D. F. Socie and G.B. Marquis, Multiaxial Fatigue. Ed. SAE International, USA. (2000).
[17] A. Varvani-Farahani, A new energy-critical plane parameter for fatigue life assessment of various metallic materials subjected to in-phase and out-of-phase multiaxial fatigue loading conditions, *International Journal of Fatigue*. **22** (2000) 295-305.
[18] A. Varvani-Farahani, Silicon MEMS components: a fatigue life assessment approach, *Microsystem Technologies*. **11** (2005) 129-134.
[19] Y. Y. Wang and W.X. Yao, Evaluation and comparison of several multiaxial fatigue criteria, *International Journal of Fatigue.* **26** (2004) 17-25.
[20] T. Itoh, M. Kameoka and Y. Obataya, A new model for describing a stable cyclic stress-strain relationship under non-proportional loading based on activation state of slip systems, *Fatigue Fract. Eng. Meter. Struct.* **27** (2004) 957-967.
[21] S. B. Lee, A criterion for fully reversed out-of-phase torsion and bending, ASTM STP 853, Philadelphia, 1985.
[22] G. I. Taylor, Plastic strain in metals, *J. Inst. Metals.* **62** (1938) 307-324.
[23] N. Jayaraman and M. M. Ditmars, Torsional and biaxial (tension-torsion) fatigue damage mechanisms in Waspaloy at room temperatures, *International Journal of Fatigue.* **11** (1989) 309-318.
[24] Y. Jiang, O. Hertel and M. Vormwald, An experimental evaluation of three critical plane

multiaxial fatigue criteria, *International Journal of Fatigue*, **29** (2007) 1490-1502.
[25] Y. Xue, D. L. McDowell, M. F. Horstemeyer, M. H. Dale and J. B. Jordon, Microstructure-based multistage fatigue modeling of aluminum alloy 7075-T651, *Engineering Fracture Mechanics.* **74** (2007) 2810-2823.
[26] R. von Mises, Mechanik der festen körper im plastisch deformablen zustand, *Math. Phys.* 1 (1913) 582-592.
[27] J. L. Chaboche, Constitutive equations for cyclic plasticity and cyclic viscoplasticity, *International Journal of Plasticity*. **5** (1989) 247-302.
[28] ANSYS Theory Reference, ANSYS Documentation, Axisymmetric Shells (11.4.1.). ANSYS Inc. (2015).
[29] J. Hoffmeyer, R. Döring, T. Seeger and M. Vormwald, Deformation behavior, short crack growth and fatigue lives under multiaxial non-proportional loading, *International Journal of Fatigue.* **28** (2006) 508-520.
[30] C. M. Sonsino, Influence of load and deformation-controlled multiaxial tests on fatigue life to crack initiation, *International journal of Fatigue.* **23** (2001) 159-167.
[31] FKM (Forschungskuratorium Maschinenbau), Analytical Strength Assessment of Components, VDMA Publ., 6th revised edition (2012).